PHYSICAL REVIEW B VOLUME 8, NUMBER 12 15 DECEMBER 1973

# Energy Levels of Iron and Aluminum in $SrTiO_3$

F. J. Morin and J. R. Oliver
*Science Center, Rockwell International, Thousand Oaks, California 91360*

(Received 4 June 1973)

An attempt is made to locate the energy levels associated with iron and aluminum in the band gap of $SrTiO_3$. A relative energy-level scheme for these impurities is derived from data in the literature, principally ESR and optical absorption. Measurements of thermally stimulated current, electrical conductivity, and thermoelectric effect are reported in this paper. These results suggest specific energy-level assignments as follows: oxygen-ion-vacancy donors 0.085 eV below the conduction band; $Al^{3+}$ acceptor, 0.18 eV; $Fe^{5+}$ acceptor, 0.75 eV; $Fe^{4+}$ acceptor, 1.06 eV; and $Fe^{3+}$-vacancy acceptor 1.35 eV above the valence band. Other levels whose identities are unknown are acceptors at 0.50 and 0.65 eV from the valence band and a donor 0.35 eV from the conduction band. The possibility is discussed that the acceptor $Fe^{3+}$ vacancy acts to couple the bound-free vacancy equilibrium to the electron-hole equilibrium.

## I. INTRODUCTION

The possible utility of $SrTiO_3$ as a model material with which to study $d$-band surface states was suggested in previous papers.[1,2] Prior to such a study, however, some knowledge was required concerning the energies of bulk states introduced into the band gap by background impurities and lattice defects. Very little information of this kind exists for $SrTiO_3$. Furthermore, nearly all of the experimental literature on $SrTiO_3$ has depended upon a single commercial source of crystals. Accordingly, in order to obtain a preliminary view of the electrical properties of this material, we have made measurements of thermally stimulated current, electrical conductivity, and thermoelectric effect on insulating crystals of commercial $SrTiO_3$.

Aluminum and iron are the major electrically active background impurities. They enter the lattice as $Al^{3+}$ and $Fe^{3+}$ substituting for $Ti^{4+}$ and bring with them oxygen-ion vacancies which preserve lattice neutrality. The transport processes which result from these defects can be quite complex. Iron, which can exist in several valence states, introduces a set of energy levels spread across the band gap. The iron-vacancy complex introduces an additional set of energy levels. The condition of electrical neutrality produced by the growth process is such that the Fermi level lies in the lower half of the band gap. However, vacancies are thermally liberated from the aluminum-vacancy and iron-vacancy complexes with the result that vacancy transport dominates hole transport over a wide temperature range in the as-grown undoped crystal. A further complication of the transport behavior appears to occur because the iron-vacancy complex, which can act both as a source of mobile vacancies and as an electronic energy level, couples the bound-free vacancy equilibrium to the electron-hole equilibrium.

In this paper we shall make use of data from the literature together with our transport measurements to construct a tentative energy-level scheme for aluminum and iron in $SrTiO_3$. In a subsequent paper we plan to describe measurements of vacancy transport and of phenomena associated with coupled electron-vacancy equilibria.

## II. BACKGROUND

The dominant electrical impurities in commercial $SrTiO_3$ are aluminum and iron. In the as-grown crystal they are present largely as $Al^{3+}$ and $Fe^{3+}$ substituting for $Ti^{4+}$. Electrical neutrality is maintained by the presence of oxygen-ion vacancies which are associated with approximately one-half of the impurity ions. Electron-spin-resonance (ESR) and optical-absorption studies are primarily responsible for knowledge of these defect centers and of the changes produced in them by oxidation, reduction, thermal quenching, and band-gap illumination. The energy-level scheme shown in Fig. 1 has been derived from these studies. It shows the energy levels due to aluminum and iron we expect to find in the ~3-eV band gap of $SrTiO_3$. The Fermi level in Fig. 1 is at the top of the valence band and the levels which we shall describe are drawn as being empty.

Oxygen-ion vacancies can be expected to produce energy levels near the conduction band which act as donors and as electron traps. The aluminum-vacancy complex, for example, may be written $Al^{3+}VTi^{3+}$ when neutral. In this representation, $Al^{3+}$ and $Ti^{3+}$ are located in adjacent oxygen octahedra which share a corner. The corner is occupied by an oxygen-ion vacancy. This donor can ionize to deliver a single electron into the conduction band by the reaction

$$Al^{3+}VTi^{3+} \rightarrow Al^{3+}VTi^{4+} + e \ .$$

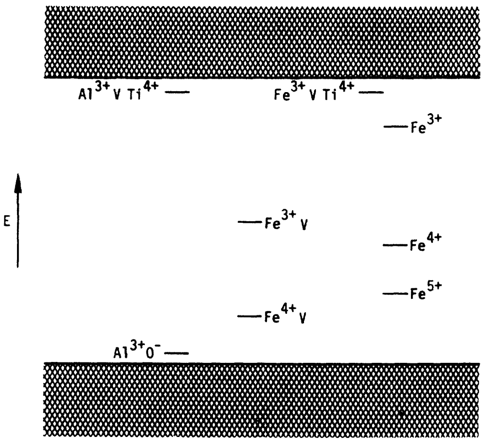

FIG. 1. Energy-level scheme for iron and aluminum in $SrTiO_3$.

$Fe^{3+}VTi^{3+}$ also forms a similar donor center. The location of the electron within the center has not been determined. We have assumed it to be on the titanium since we expect the presence of the vacancy to lower the Madelung potential at the titanium site and split a level from the conduction band. Another vacancy donor, not shown in Fig. 1, is the double donor $Ti^{3+}VTi^{3+}$ which is introduced into the crystal by reduction. In transport studies on reduced crystals,[3,4] a temperature dependence was observed for conduction-electron concentration which indicated an ionization energy of 0.08 eV for one of the levels of $Ti^{3+}VTi^{3+}$. ESR studies[5] on insulating $SrTiO_3$ indicate the presence of an electron trap which is stable at 77 °K but not at 300 °K. This result suggests a trap, which may be associated with the vacancy centers, within a few tenths eV from the conduction band.

Aluminum is expected to introduce an acceptor level which, when neutral, may be written as $Al^{3+}O^-$. ESR studies[6] indicate that the hole, shown on the oxygen in this representation, is shared by the oxygen octahedra which surrounds the aluminum The center also has been seen to act as a hole trap which empties above ~ 100 °K. This process may be represented by the reaction

$$Al^{3+}O^- \rightarrow Al^{3+}O^{2-} + h \ .$$

The low temperature at which the trap empties suggests that it is within a few tenths eV from the valence band as shown in Fig. 1. The analogous hole trap $Fe^{3+}O^-$ is not expected to exist because the acceptor level $Fe^{3+}O^-$ probably lies below the $Fe^{4+}O^{2-}$ level for iron and will be filled by the reaction

$$Fe^{3+}O^- \rightarrow Fe^{4+}O^{2-} \ .$$

Furthermore, no resonance signal has been seen which could be associated with the hole in $Fe^{3+}O^-$.

Iron plays a much more complex role than does aluminum because, in addition to associating with vacancies, it can occur in several valence states. ESR and optical absorption have indicated[5-8] the presence of iron in the valence states 2+, 3+, 4+, and 5+. These states are represented by the three empty levels shown in Fig. 1 as being spread across the band gap. They may be filled by electrons according to the reactions

$$Fe^{5+} \rightarrow Fe^{4+} + h \ ,$$

$$Fe^{4+} \rightarrow Fe^{3+} + h \ ,$$

$$Fe^{3+} \rightarrow Fe^{2+} + h \ .$$

A second set of levels is also to be expected from the iron-vacancy complex. These levels are shown empty in Fig. 1 and may be filled by the reactions

$$Fe^{4+}V \rightarrow Fe^{3+}V + h \ ,$$

$$Fe^{3+}V \rightarrow Fe^{2+}V + h \ .$$

The energy level for an iron-vacancy complex associated with a particular valence state of iron is shown to be lower than the corresponding level for the same valence state but with no vacancy. This is because the Madelung potential is lowered on the cation site next to a vacancy. A level is not shown for $Fe^{5+}V$ because it would appear to be a very unstable complex. An axial ESR signal has been identified with $Fe^{3+}V$ but neither $Fe^{2+}V$ nor $Fe^{4+}V$ have been detected. Since the center $Fe^{3+}VTi^{4+}$ has a net positive charge, it is a possible electron trap but with the electron on the $Fe^{3+}$ rather than on the $Ti^{4+}$ as discussed above. The $Fe^{3+}V$ signal is seen to disappear at the same rate that $Fe^{4+}$ is generated from $Fe^{3+}$ with band-gap illumination and to reappear when $Fe^{3+}$ is reformed by bleaching.[6] This result suggests the possibility that the electron is being trapped according to the reaction

$$Fe^{3+} + Fe^{3+}V \rightarrow Fe^{4+} + Fe^{2+}V.$$

The ESR and optical-absorption results suggest where the Fermi level might be drawn in Fig. 1. We know that iron is present as $Fe^{3+}$ and $Fe^{3+}V$ in the as-grown crystal. This implies that the Fermi level is between the $Fe^{4+}$ and $Fe^{3+}V$ levels so that the former is full and the latter is empty. Oxidation, which increases the $Fe^{4+}$ concentration, moves the Fermi level down into the $Fe^{4+}$ level. Irradiation with band-gap light produces a trapped hole[6] which has been identified[7] as $Fe^{5+}$ and which is stable at 300 °K. This places the $Fe^{5+}$ level at least a factor of 3 deeper into the band gap than the aluminum hole trap which empties at ~ 100 °K. The $Fe^{5+}$ resonance increases in intensity when the crystal is doped with additional aluminum, another indication that the $Fe^{5+}$ level lies above the $Al^{3+}O^-$ level as shown in Fig. 1.

The $Fe^{5+}$ state is also produced[6] when the crystal is cooled rapidly from 1200 °C in oxygen. This observation, together with the fact that the $Fe^{5+}$ trapped hole is stable at 300 °K, suggests the presence of a stable, and therefore deep, electron trap. If we assume that the deep trap is $Fe^{3+}V$ then the reaction which produces $Fe^{5+}$ with thermal quenching or optical excitation must be

$$Fe^{4+} + Fe^{3+}V \rightarrow Fe^{5+} + Fe^{2+}V .$$

Therefore, the production of $Fe^{5+}$ depends upon the location of the Fermi level, for if half of the iron is present as $Fe^{3+}$, then the reaction becomes

$$Fe^{3+} + Fe^{3+}V \rightarrow Fe^{4+} + Fe^{2+}V ,$$

and the $Fe^{5+}$ is not produced. This may be the situation in iron-doped crystals where it was observed that $Fe^{5+}$ could not be produced by optical excitation or by quenching from elevated temperatures.[6]

So far in this section we have been considering the electronic properties of $SrTiO_3$. Studies of electrocoloration[9] have shown, however, that oxygen-ion vacancies may make a significant contribution to conductivity at temperatures above ~400 °K. The vacancies that we have to contend with, as pointed out above, are brought into the lattice to compensate the deficiency of positive charge on 3+ impurity ions. High-temperature measurements of the oxygen-ion self-diffusion coefficient[10] show that it is independent of oxygen pressure. This suggests that the concentration of vacancies introduced with the 3+ ion impurities exceeds the concentrations associated with equilibrium stoichiometry. Thus heating the crystals in various partial pressures of oxygen can be expected to change the relative amounts of donors and acceptors and thus the Fermi level, for example, by the reaction

$$Al^{3+}O^{2-} + Al^{3+}V + 0.5\ O_2(\text{gas}) \rightarrow 2Al^{3+}O^- ,$$

but will not eliminate vacancies from the lattice. This result is important to our experiments in which we found that vacancy transport could be suppressed by oxidation to allow hole transport to be studied. Oxidation did not significantly reduce total vacancy concentration, however, with the result that coupled hole-vacancy equilibria were still present to complicate hole transport.

## III. EXPERIMENTAL

Samples from six boules of $SrTiO_3$ were studied.[11] Three boules were nominally undoped and the remaining three were doped, respectively, with aluminum, iron, and vanadium. Solid mass-spectrographic analysis for the major impurities is shown in Table I. The background impurity levels of the doped crystals were assumed to be those shown in Table I for $B3$ except that in the case of the aluminum-doped crystal molybdenum was inadvertently added and in the case of the vanadium-doped crystal aluminum was inadvertently added. Vanadium was chosen as a dopant after experiments on undoped crystals showed the Fermi level to lie in the lower-half of the band gap. It was hoped that the addition of vanadium, a donor, would move the Fermi level into the upper-half of the band gap and thus facilitate the study of defect levels in that energy region. The addition of aluminum with the vanadium prevented this.

Sample specimens were 10×2×1 mm cut parallel to the cubic axes of the perovskite lattice. Mechanical damage was removed by etching in hot phosphoric acid. Contacts were made using Hanovia liquid gold cured in air at ~600 °C for approximately 60 sec. Gold, rather than the frequently used gallium-indium alloy, was used for contacts to permit measurements to be made at high temperature. Gold on $p$-type $SrTiO_3$ meets the requirement for Ohmic contacts, namely, that the work function of the metal be less than that of the insulator. The gold contacts on our material gave linear current-voltage characteristics over a wide range of voltage and temperature. The work function of indium-gallium against $SrTiO_3$ is about one-third that of gold.[12] Contacts of indium-gallium alloy gave current-voltage characteristics at room temperature identical to those found for gold. In addition, a four-point-potential-probe measurement of conductivity, using gold contacts, was made on a sample of oxidized undoped $SrTiO_3$ over the temperature range 300–1100 °K. The results were the same as those obtained with a two-point conductivity measurement. Consequently, the measurements reported in this paper made use of only two contacts in order to simplify sample-holder design.

The low-temperature sample holder permitted operation between 55 and 500 °K with a gas or a

TABLE I. Mass-spectrographic analysis of the major impurities in $SrTiO_3$ crystals (atomic parts per million).

| Impurity | $B1$ | $B2$ | $B3$ | $B4$ | $B5$ | $B6$ |
|---|---|---|---|---|---|---|
| Al | 10 | 8 | 6 | 600 | | 150 |
| Fe | 25 | 20 | 30 | | 80 | |
| W | 15 | 2.5 | 0 | | | |
| Cr | | 4.0 | <1 | | | |
| Na | 46 | 7.0 | 32 | | | |
| Si | 16 | | | | | |
| Cl | 35 | 70 | 44 | | | |
| Mo | | | | 34 | | |
| V | | | | | | 72 |

mechanical-pump vacuum as ambient atmosphere. The sample was supported between two heated blocks which permitted heating-rate control, typically 0.1 °K/sec, and the establishment of a temperature gradient along the length of the sample. The design was intended to permit measurement of the sign but not the absolute magnitude of the thermoelectric effect. The sample was illuminated with light obtained from a halogen-tungsten lamp and passed through a Corning 7-59 filter. Sample current was generated by a constant-voltage supply and detected with an electrometer and a logarithmic amplifier and recorded continuously on semilog paper against thermocouple voltage. The applied field was typically 1 V/cm. The high-temperature sample holder permitted operation between 300 and 1600 °K with a gas ambient. A small heater permitted a temperature gradient to be established along the sample for measurement of the sign of the thermoelectric effect. Sample current was maintained at sufficiently low levels that the accumulation of vacancies at the cathode and oxygen ions at the anode was minimized.

In the analysis of the results to follow, the location of the Fermi level is assumed to be given to a good approximation by the slope of the curves of log conductivity versus reciprocal temperature. This assumption ignores the possible temperature dependence of carrier mobility. However, for our purposes this is a reasonable assumption since the effect of mobility is important only at the lowest temperature of our measurement where our probable error is an over estimate of the energy of the Fermi level by about 10%.

## IV. THERMALLY STIMULATED CURRENT RESULTS

We saw in Sec. II that the centers $\mathrm{Al}^{3+}V\mathrm{Ti}^{4+}$, $\mathrm{Fe}^{3+}V\mathrm{Ti}^{4+}$, and $\mathrm{Ti}^{4+}V\mathrm{Ti}^{4+}$ are expected to act as electron traps which empty between 77 and 300 °K. Also, the center, $\mathrm{Al}^{3+}\mathrm{O}^{2-}$, is expected to act as a hole trap which empties in the same temperature range. It was found, in fact, that in some of the crystals, the concentrations of electron and hole traps were comparable and, consequently, that the thermally-stimulated-conductivity TSC peaks from these two sets of traps overlapped. It was fortunate that in crystal *B*1 the electron traps predominated as did the hole traps in crystal *B*3 so that they could be studied separately.

A plot of TSC from a *B*1 sample is shown in Fig. 2. In this experiment, the current was due predominately to electrons and peaked at 92 °K. The series of straight lines in Fig. 2 were produced by a repeat of the TSC experiment but with successive warming and cooling cycles which emptied the band of trap states a few $kT$ per cycle.[13,14] This result indicates a spread in electron trap energy of ~ 0.3 eV beginning somewhat below 0.08 eV and peaking at ~ 0.085 eV below the conduction band. This was the major band of electron traps found between 77 and 300 °K, so it seems reasonable to associate it with the $\mathrm{Al}^{3+}V\mathrm{Ti}^{4+}$ type of center.

A plot of TSC from a *B*3 sample is shown in Fig. 3. In this experiment the hole current predominated in two temperature regions and peaked at 148 and 480 °K. These peaks correspond to a band of traps centered at 0.18 eV and another at 0.75 eV above the valence band. It seems reasonable to associate these traps with the centers $\mathrm{Al}^{3+}\mathrm{O}^{-}$ and $\mathrm{Fe}^{5+}$, respectively, since the former has been seen to decay above 100 °K and the latter is reported as being stable at 300 °K. Between 200 and 300 °K in Fig. 3, the current was due predominately to electrons from a trap 0.3 – 0.4 eV below the conduction band. We have often seen a small TSC peak at 250 °K in other crystals but have been unable to identify it with a specific impurity. The background current due to bulk conductivity is shown at the far left of Fig. 3. It has a slope of 1.10 eV, is $n$ type, and is believed due to oxygen-ion vacancies.

## V. ELECTRICAL–CONDUCTIVITY RESULTS

The dark electrical conductivity of an as-grown *B*2 sample is shown in Fig. 4. Three regions of transport can be distinguished. Below 450 °K, the

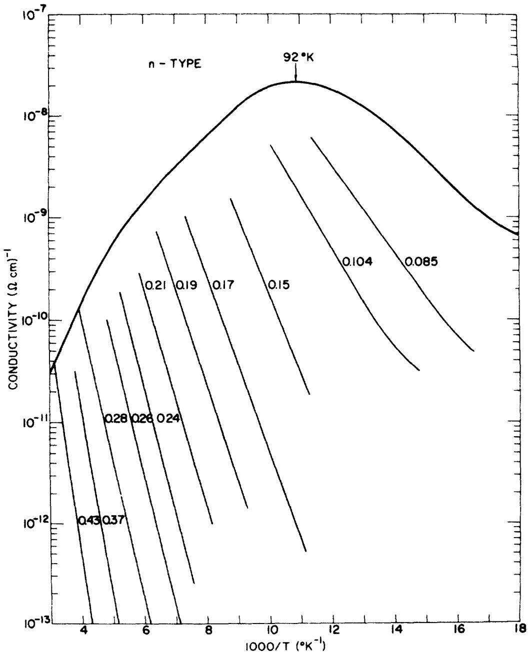

FIG. 2. Thermally stimulated conductivity vs reciprocal absolute temperature for an as-grown sample from crystal *B*1.

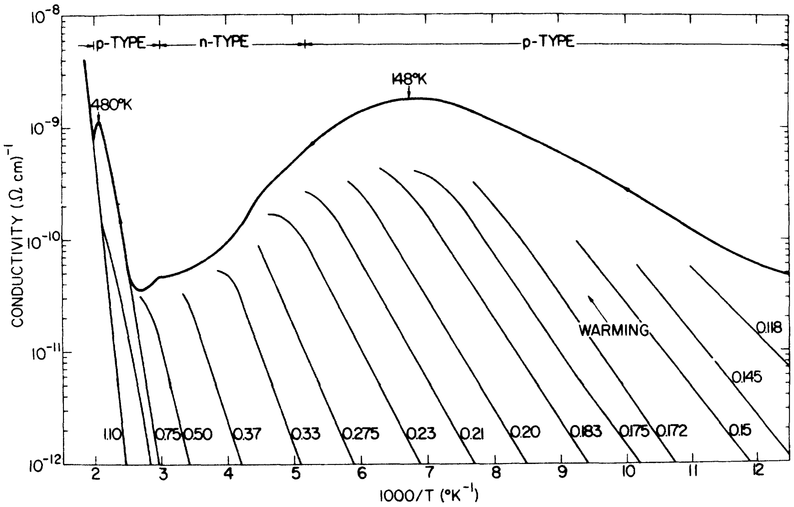

FIG. 3. Thermally stimulated conductivity vs reciprocal absolute temperature for an as-grown sample from crystal *B*3.

conductivity is *p* type with a slope of ~ 0.5 eV. From its behavior, it is clear that the conductivity in this temperature region is due to trapped holes which are being thermally liberated since the conductivity is less on cooling than on initial warming. The trap becomes partially occupied in the dark at room temperature and empties at ~ 380 °K. An indication of its presence at 0.50 eV is seen in Fig. 3. Between 450 and 650 °K, the sample in Fig. 4 shows *n*-type conductivity with a slope of 1.10 eV. Experiments to be described in another paper together with the work on vacancy transport[9] allow us to identify this region as being due to oxygen-ion vacancy transport. Above 650 °K, conductivity again becomes *p* type. It also shows a tendency to saturate and hysteresis which depends upon the heating and cooling rates of the measurement. Thus, vacancy transport gives way to hole transport at high temperature and the hole transport appears to be due to an acceptor complex whose concentration is temperature-time dependent. The results in Fig. 4 were obtained in an atmosphere of nitrogen and were quite reproducible in this atmosphere provided sample temperature remained below ~ 1100 °K. In oxygen atmosphere, the sample oxidized at temperatures as low as 900 °K and vacancy transport was sufficiently suppressed that conductivity became *p* type over the entire temperature range. Although the hysteresis region persisted in the oxidized samples, below this region the temperature dependence of conductivity appeared to provide a reliable indication of the location of the Fermi level.

Conductivity is shown in Fig. 5 for a set of samples which were doped to move the Fermi level and oxidized to suppress vacancy transport. All of the samples were *p* type. The slopes of these curves show that the Fermi level was moved down to 0.68 eV above the valence band by doping with the acceptor, aluminum and raised to 1.35 eV above the valence band by doping with the donor, vandium. Following the discussion in Sec. II, we expect the Fermi level in an undoped crystal and in an iron-doped crystal to lie on the $Fe^{4+}$ level when the crystal is oxidized. From the slopes of the conductivity curves in Fig. 5 for undoped and iron-doped samples, we infer that the $Fe^{4+}$ level lies ~ 1.0 eV above the valence band. We also saw in Sec. II that the addition of aluminum converted the background impurity iron to $Fe^{5+}$. For this reason, we expected the conductivity curve for the aluminum-doped sample to confirm the assignment made in Sec. IV of 0.75 eV for the $Fe^{5+}$ level. We find that the Fermi level in the aluminum-doped sample lies at 0.68 eV, or somewhat below the expected energy. However, the result for the aluminum-doped sample confirms that a high concentration of acceptor levels, probably due in part to $Fe^{5+}$, exists in the vicinity of 0.7 eV above the valence band. Conductivity for the vanadium-doped sample shown in Fig. 5 shows the Fermi level to be 1.35 eV above the valence band. At present, the only candidate for this level is $Fe^{3+}V$ as shown in Fig. 1.

Following the discussion in Sec. II, we expect that $Fe^{5+}$ will be produced from background impurity iron by a quick quench from an elevated temperature. The conductivity curves in Fig. 6 show the results of this experiment. Curve (a) in Fig. 6 shows the typical behavior on heating and cooling for the conductivity of an oxidized undoped sample from *B*3. The 0.5-eV hole trap is in evidence, emptying ~ 380 °K. The Fermi level lies on the 1.0-eV $Fe^{4+}$ level up to ~ 550 °K and above this temperature we see the hysteresis region. When this sample was quenched in a few seconds from

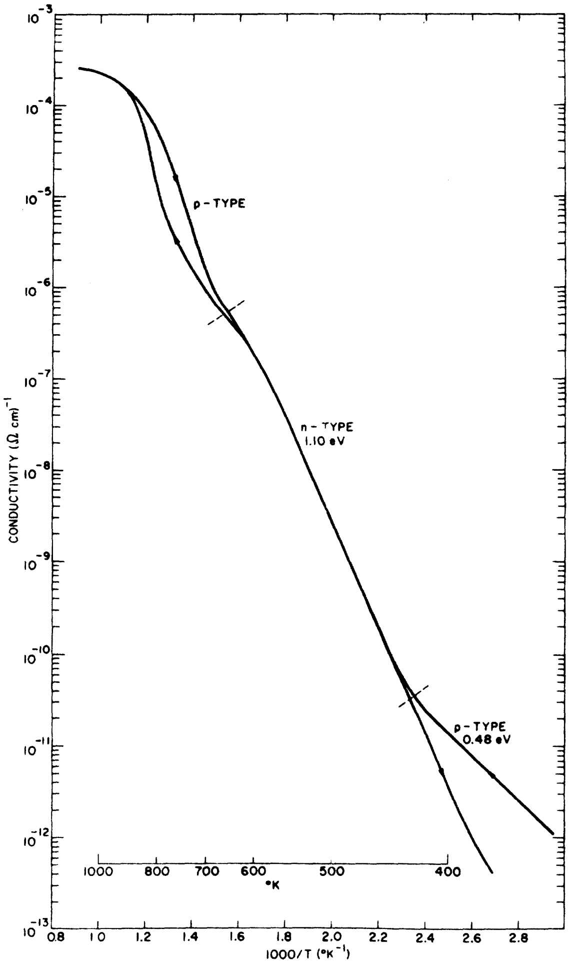

FIG. 4. Electrical conductivity vs reciprocal absolute temperature for an as-grown sample from crystal *B*2.

950 °K to room temperature in oxygen, the conductivity shown by curve (b) in Fig. 6 resulted. After the quench, the warming curve shows enhanced conductivity which has a slope of 0.72 eV. The conductivity peaks at 630 °K and then drops to what appears to be the 1.35-eV level seen before in Fig. 5. The conductivity then rejoins the original curve (a) and follows it down on cooling. The entire process was found to be reproducible. The 0.72-eV slope is consistent with the observation that the quench treatment produces $Fe^{5+}$ and our identification of this level with the 0.75-eV hole trap. However, the conductivity peak temperature of 630 °K is not consistent with the observation in Fig. 3 that this hole trap emptied at 480 °K. Rather, the result in Fig. 6 suggests that the $Fe^{5+}$ in the quench experiment acts as an acceptor level produced when electrons are removed from $Fe^{4+}$ and trapped in a deep electron trap. The conductivity then decreases abruptly when the electron trap empties at 630 °K. The thermal quench was found to have produced no essential change in conductivity of the iron-doped sample in agreement with the results quoted in Sec. II.

## VI. DISCUSSION

Our measurements have detected a number of energy levels in the band gap of commercial $SrTiO_3$ which appear to be due to the presence of aluminum and iron. These levels have been identified with specific centers in a way that is consistent with the findings of electron-spin resonance and optical spectroscopy. More positive identification would require considerable additional work. A band of electron traps ~ 0.3-eV wide has been found which has its highest density ~ 0.09-eV below the conduction band. We have identified these levels as coming from the donor centers $Al^{3+}VTi^{4+}$, $Fe^{3+}VTi^{4+}$, and $Ti^{4+}VTi^{4+}$. A band of hole traps identified with the acceptor $Al^{3+}O^-$ has been found centered ~ 0.18 eV above the valence band. Two deeper acceptor levels have been found which appear to be due to different valence states of iron: $Fe^{5+}$ at 0.75 eV and $Fe^{4+}$ at 1.06 eV above the valence band. The other energy levels associated with iron and shown in Fig. 1 cannot be identified with as much confidence. If $Fe^{3+}V$ is sufficiently stable against dissociation

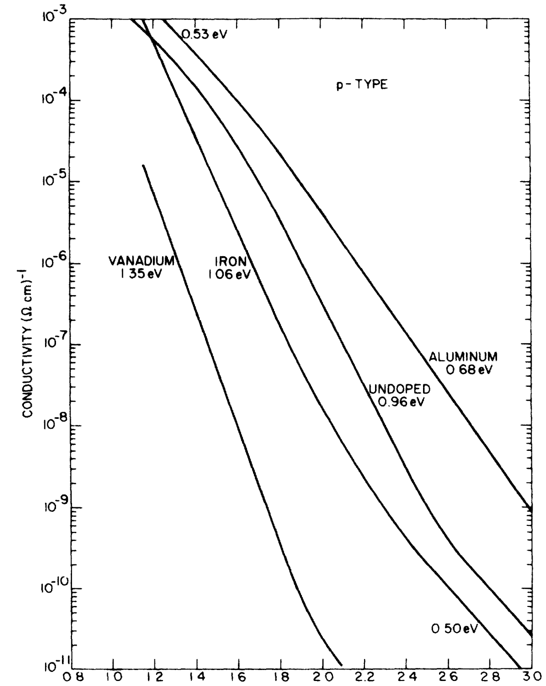

FIG. 5. Electrical conductivity vs reciprocal absolute temperature for oxidized samples from crystal *B*3 (undoped), *B*4 (aluminum doped), *B*5 (iron doped), and *B*6 (vanadium and aluminum doped).

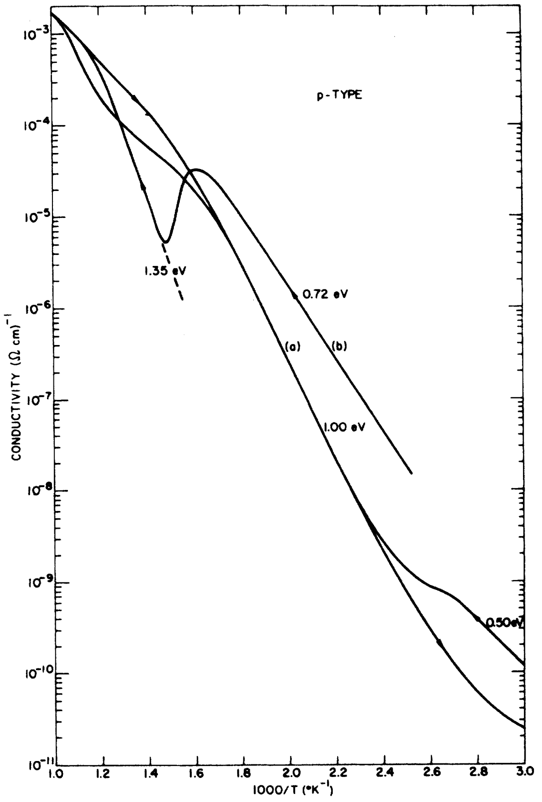

FIG. 6. Electrical conductivity vs reciprocal absolute temperature for (a) an oxidized sample from crystal *B*3, (b) the same sample after a thermal quench from 950 °K in oxygen.

into $Fe^{3+}$ and free vacancy then it is a candidate for the 1.35-eV level and, consequently, for participation in the coupled equilibria described below. The level associated with $Fe^{3+}$ is probably in the region of the upper-half of the band gap which we have not explored. Several other energy levels, much less prominant than those described above, have been detected in numerous experiments. Chromium is an impurity in commercial $SrTiO_3$ in sufficient amounts to have been detected. Chromium might be expected to introduce a set of levels analogous to those of iron but displaced to higher energies. The 0.5-eV hole trap which we have seen repeatedly may be due to $Cr^{6+}$. We have also seen the Fermi level pinned between 0.65 and 0.70 eV in many experiments designed to expose the 0.75-eV level of $Fe^{5+}$: for example, the aluminum-doped experiment in Fig. 5. Our findings suggest that a high density of levels exist in the vicinity of 0.65 eV. These may be due to $Cr^{5+}$.

The hysteresis effects which have been observed repeatedly in the conductivity between 600 and 1000 °K suggest a diffusion-limited process. A possible model for the process is provided by the following set of coupled equilibria:

$$\begin{array}{ccc} & & \mathrm{Fe}^{4+} \\ & & \updownarrow \\ \mathrm{Fe}^{3+}V & \leftarrow & \mathrm{Fe}^{3+} + V \\ \updownarrow & & + \\ \mathrm{Fe}^{2+}V & & h \\ + & & \\ h & & \end{array}$$

Coupled equilibria of this kind appear to be likely in $SrTiO_3$ because iron exists in several valence states and associates with vacancies. The horizontal reaction represents the bound-free vacancy equilibrium involving iron. Vacancies will also be supplied to this equilibrium by the similar equilibrium which involves aluminum. The vertical reaction on the right shows the transfer of an electron from the valence band into the $Fe^{4+}$ acceptor level to create $Fe^{3+}$ and a hole. The other vertical reaction represents the transfer of an electron from the valence band into the $Fe^{3+}V$ acceptor level to create $Fe^{2+}V$ and a hole. Since the binding energy for the vacancy complex increases in the sequence $Fe^{4+}V$, $Fe^{3+}V$, $Fe^{2+}V$, we may expect that the transfer of electrons into the acceptor levels with increasing temperature will move the equilibria to the left and increase the concentration of the $Fe^{2+}V$ acceptor. Qualitatively, this model can account for the transition with increasing temperature from vacancy transport to hole transport seen in Fig. 4. It also accounts for a hysteresis loop in which conductivity is higher on cooling than on warming. Also, as predicted, the absence of $Fe^{4+}$ together with a higher concentration of vacancies in the unoxidized sample, Fig. 4, produces a steeper conductivity slope in the hysteresis region than found in the oxidized sample curve (a), Fig. 6. If the model is correct, one would expect it to play an important role in the quench experiment. When the sample is equilibrated at elevated temperature, a large concentration of $Fe^{2+}V$ and of holes in the valence band must be built up which are quenched in when the sample is rapidly cooled. The model does not explain how the $Fe^{3+}$ ions which probably exist under these conditions, trap two holes to become $Fe^{5+}$ ions.

---

[1] T. Wolfram, E. A. Kraut, and F. J. Morin, Phys. Rev. B 7, 1677 (1973).

[2] F. J. Morin and T. Wolfram, Phys. Rev. Lett. 30, 1214 (1973).

[3] O. N. Tufte and P. W. Chapman, Phys. Rev. **155**, 796 (1967).

[4] C. Lee, J. Yahia, and J. L. Brebner, Phys. Rev. B **3**, 2525 (1971).

[5] B. W. Faughnan, Phys. Rev. B **4**, 3623 (1971).

[6] T. C. Ensign and S. E. Stokowski, Phys. Rev. B **1**, 2799 (1970).

[7] K. A. Müller *et al.*, Solid State Commun. **9**, 1097 (1971).

[8] R. L. Wild, E. M. Rockar, and J. C. Smith, Phys. Rev. B **8**, 3828 (1973).

[9] J. Blanc and D. L. Staebler, Phys. Rev. B **4**, 3548 (1971).

[10] A. E. Paladino, L. G. Rubin, and J. S. Waugh, J. Phys. Chem. Solids **26**, 391 (1965).

[11] Boule *B*1 was obtained from Electronic Space Products, Inc., Los Angeles, Calif.; the remaining boules were obtained from N. L. Industries, N. J., the source for nearly all of the crystals reported on in the literature.

[12] J. E. Carnes and A. M. Goodman, J. Appl. Phys. **38**, 3091 (1967).

[13] R. H. Bube *et al.*, J. Appl. Phys. **37**, 21 (1966).

[14] W. C. Mallard and J. H. Crawford, J. Appl. Phys. **43**, 2060 (1972).